

Rician 페이딩 채널에서 최적검파 및 선택합성 다이버시티 기법을 도입한 16 QAM 신호의 오율 특성

(Error Performance of 16 QAM Signal with Optimum Threshold Detection and SC Diversity Techniques in Rician Fading Channel)

김 언 곤* · 고 봉 진** · 조 성 준***

(Eon Gon Kim*, Bong Jin Ko**, Sung Joon Cho***)

요 약

본 논문에서는 Rician 페이딩 채널에서 16 QAM 신호에 대한 최적 검파(OTD) 기법을 제안하고 선택 합성 다이버시티를 도입할 때와 도입하지 않을 때 16 QAM 신호에 대한 최적 검파(OTD)시의 오율 성능을 해석하였다. 그리고 최적 검파(OTD)의 오율 성능을 기존의 검파(CTD)시의 오율 성능과 비교하였다.

선택 합성 다이버시티 수신을 행할 경우, 오율이 10^{-5} 이고 페이딩 심도의 값 K가 5에서 30까지 변할 때 본 논문에서 제안하는 최적 검파(OTD) 기법이 기존의 검파(CTD)시보다 CNR면에서 1.8~3.2[dB]의 성능개선이 있었다.

수치 해석 결과로부터, 제안하는 최적 검파(OTD)의 성능이 기존의 검파(CTD)에 비해 Rician 페이딩 채널에서 우수하고, 최적 검파에 선택 합성 다이버시티 기법을 도입하면 Rician 페이딩에 대해 우수한 대응책이 되리라는 것을 알 수 있었다.

Abstract

We have proposed the optimum threshold detection(OTD) technique of 16 QAM signal in the Rician fading channel and analyzed its error performance with and without the selective combining(SC) diversity technique. And we compared the error performance of OTD with that of conventional threshold detection(CTD).

Having the SC diversity reception, optimum threshold detection(OTD) technique proposed in this paper provides the performance improvement of 1.8~3.2[dB] in CNR for fading depth K values

* 삼성전자(주) 통신연구소 무선통신그룹
Wireless Comm. Group, Telecomm. R&D Center, Samsung Electronics
** 인하공업전문대학 통신과
Dept. of Comm. Eng., Inha Technical Junior College
*** 한국항공대학교 항공통신정보공학과
Dept. of Telecomm. and Infor. Eng., Hankuk Aviation University

ranging from 5 to 30 over CTD when the error rate is 10^{-5} .

From the result of numerical analysis, we know that the proposed OTD technique is superior to CTD technique in the Rician fading channel and adoption of the SC diversity technique with the proposed OTD can be considered as a good countermeasure for the Rician fading.

I. INTRODUCTION

Recently, there is a great demand for mobile services and personal communication services. To keep up with the demand, the development and standardization in these services are progressed in several countries [1], [2].

There are two interim approaches toward the ultimate goal, the personal communication services: the cordless systems and the cellular systems. They both have an option for the personal communication services in a limited manner and they are expected to merge together to form the personal communication services [3].

In the personal communication systems which require a high channel capacity and limited bandwidth usage, a multi-level modulation method is desirable. The 16 QAM is a very attractive multi-level modulation technique in terms of the power and frequency efficiency [4]. However, 16 QAM has a poor error rate performance in a fading channel due to its inherent nature of having different levels for different symbols, therefore TCM and equalization techniques are proposed as the performance improvement [4], [5].

Conventionally, the threshold levels for detecting the QAM symbols are equi-distance regardless of the magnitude of the QAM signal. However, the degree of fading is proportional to the ratio of the direct-to-diffuse signal power. Thus, the threshold levels for detecting the QAM symbols must be adjusted accordingly. In this paper,

we analyze the performance of the optimum threshold detection(OTD) of 16 QAM signal in the Rician fading channel with and without selective combining(SC) diversity technique.

The rest of the paper is organized as follows. In Chapter II, the analysis model including channel is described. In Chapter III, the performance of CTD and OTD of 16 QAM signal without diversity is evaluated. Chapter IV deals with the performance improvement made with the SC diversity technique. Finally, Chapter V concludes that the 16 QAM with OTD and SC diversity technique is a good multi-level MODEM technique for the micro-cellular systems.

II. ANALYSIS MODEL

Fig. 1 illustrates the schematic diagram of the analysis model. Passing through the Rician fading channel, the modulated 16 QAM signal is corrupted by multipath fading resultant from receiving of a direct component and random diffuse components.

This fading imposes random amplitude and phase onto the modulated 16 QAM signal. Besides fading, the transmitted signals are also corrupted by

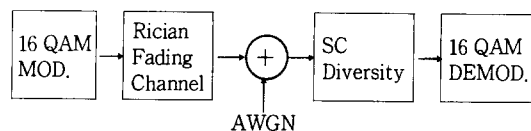


[Fig. 1] Analysis model

additive white Gaussian noise(AWGN). The received signals disturbed by Rician fading and AWGN in each diversity branch are selected and combined by diversity circuit. Diversity reception is usually regarded as a means of combating fading in radio transmissions. In SC diversity which is the simplest method of space diversity, for instance, several antennas are used, separated in space to process the various received signals and the one of the M receivers having the highest signal to noise ratio(SNR) is connected to the demodulator. The basic idea behind the concept is that the received signals on different antennas are statistically independent and therefore there is a good chance that they will not all fade at the same time. While other methods of achieving diversity are known [6], here we shall deal only with SC diversity.

The output signal from the SC diversity process is delivered to the 16 QAM demodulator. In the 16 QAM demodulator, we adopted adaptive threshold detection which is controlled by the direct-to-diffuse signal ratio.

The modulated 16 QAM signal can be expressed as [7]

$$s_{16QAM}(t) = a_i(t) \cos\omega_c t + b_i(t) \sin\omega_c t \quad (1)$$

where ω_c is the angular carrier frequency, a_i and b_i are the i th in-phase (I) and quadrature (Q) components of the modulated 16 QAM signal taking on values of $\pm d/2, \pm 3d/2$. The $\{a_i\}$ and the $\{b_i\}$ are statistically independent and equally likely to have any of their four values.

Fig. 2 illustrates a 16 QAM constellation where each dot represents the position of the phasor relative to the intersection of axes marked I (for in-phase) and Q (for quadrature). In Fig. 2, the

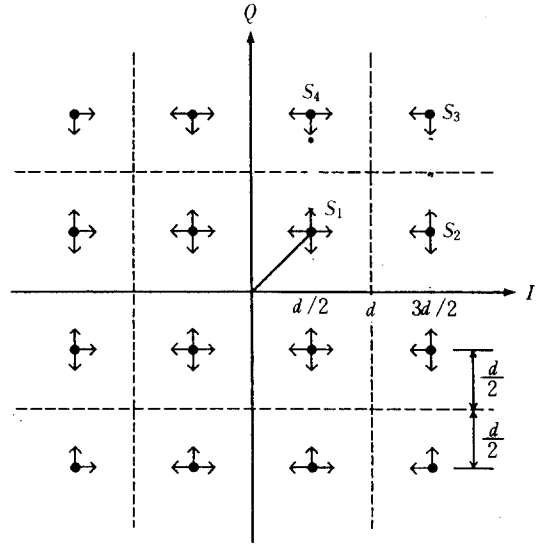


[Fig. 2] 16 QAM constellation

arrows from dots represent the error directions of the phasors. It also shows that the minimum distance between two signal points is d . In the analysis model shown in Fig. 1, the Rician fading channel is modeled as the multipath fading of a microcellular channel. In a microcellular system such as the personal communication network(PCN), the desired signal transmitted to a mobile or portable receiver will often travel over a line of sight or direct path [8], [9]. Consequently, the received signal will consist of a direct component as well as diffuse (scattered) component and its envelope will be characterized by a Rician probability density function(pdf). It is assumed that the fading varies very slowly compared to the signaling rate so that the received signal envelope is constant during one signal interval of duration T_s and there is no path loss between transmitter and receiver. The received signal power can be expressed as

$$\begin{aligned} P_{RX} &= P_{direct} + P_{diffuse} \\ &= A^2 P_{TX} + P_{diffuse}, \quad 0 \leq A^2 < 1 \end{aligned} \quad (2)$$

Deriving from Eq (2), A is $\sqrt{\frac{K}{K+1}}$ where K is a direct component to diffuse component ratio ($P_{direct}/P_{diffuse}$). The received 16 QAM signal is divided into I and Q components which are statistically independent. The I component is Gaussian distributed and its mean is equal to I component of a direct signal envelope. Fig. 3 illustrates the pdf's of the I components of the received 16 QAM signal corrupted by the Rician fading. Notice that Fig. 3 only shows the pdf's for the dots in the first quadrant of Fig. 2.

When the I components of the transmitted 16 QAM signal are $d/2$ and $3d/2$, the pdf's of I components of the received 16 QAM signal corrupted by the Rician fading are described as

$$p_1(x) = \frac{1}{\sqrt{2\pi} \sigma_1^2} \exp \left\{ -\frac{(x - A\frac{d}{2})^2}{2\sigma_1^2} \right\} \quad (3a)$$

$$p_2(x) = \frac{1}{\sqrt{2\pi} \sigma_2^2} \exp \left\{ -\frac{(x - A\frac{3d}{2})^2}{2\sigma_2^2} \right\} \quad (3b)$$

where σ_1^2 and σ_2^2 are the variances of signal points.

Since each signal of 16 QAM is transmitted in same fading channel, direct component to diffuse component ratio (K) is constant, the variance σ_2^2 is 9 times larger than σ_1^2 since the variances are proportional to signal powers.

The narrowband Gaussian noise $n(t)$ which is randomly added regardless of the transmitted signal can be expressed as [10]

$$n(t) = n_c \cos \omega_c t - n_s \sin \omega_c t \quad (4)$$

where n_c and n_s are I and Q components of $n(t)$.

Since n_c and n_s are all Gaussian distributed with zero means, their pdf's are

$$p_n(n_c) = \frac{1}{\sqrt{2\pi} \sigma_n^2} \exp \left\{ -\frac{n_c^2}{2\sigma_n^2} \right\} \quad (5a)$$

$$p_n(n_s) = \frac{1}{\sqrt{2\pi} \sigma_n^2} \exp \left\{ -\frac{n_s^2}{2\sigma_n^2} \right\} \quad (5b)$$

where σ_n^2 is the variance of $n(t)$.

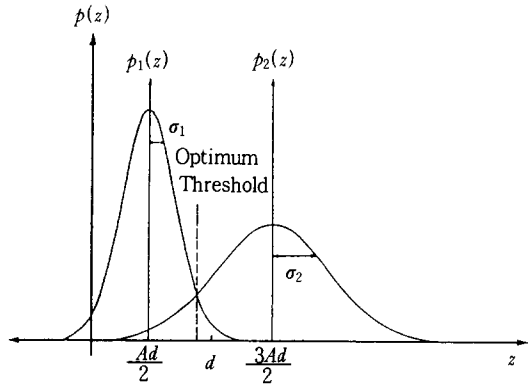


[Fig. 3] The pdf's of the I components of the received 16 QAM signal

III. PERFORMANCE ANALYSIS WITHOUT DIVERSITY

1. Conventional Threshold Detection(CTD)

I component of the received 16 QAM signal corrupted by the Rician fading is Gaussian distributed as well as the I component of noise. Thus, $p(z) = p(x + n_c)$, the pdf of the sum of them must be a Gaussian distribution[11]. When the I components of the transmitted signals are $d/2$ and $3d/2$, the pdf's are given as follows;

$$p_1(z) = \frac{1}{\sqrt{2\pi} (\sigma_1^2 + \sigma_n^2)} \cdot \exp \left\{ -\frac{(z - \frac{Ad}{2})^2}{2(\sigma_1^2 + \sigma_n^2)} \right\} \quad (6a)$$

$$p_2(z) = \frac{1}{\sqrt{2\pi} (\sigma_2^2 + \sigma_n^2)} \cdot \exp \left\{ -\frac{(z - \frac{3Ad}{2})^2}{2(\sigma_2^2 + \sigma_n^2)} \right\} \quad (6b)$$

When the I component of the transmitted 16 QAM signal is $d/2$ and the conventional threshold levels(CTL) for detecting the 16 QAM signal are 0 and d , the erroneous detection is made when the I component of the received 16 QAM signal exceeds 0 in the left direction or d in the right direction. In the case of the I component value of $3d/2$, the error occurs only if the I component of the received signal crosses the boundary d in the left direction.

The error probabilities of three cases mentioned above are defined as P_{ICA} , P_{ICB} , and P_{ICC} , respectively,

$$P_{ICA} = \int_{-\infty}^0 p_1(z) dz$$

$$= \frac{1}{2} \operatorname{erfc} \left[\sqrt{\gamma \frac{K}{5(1+K) + \gamma}} \right] \quad (7a)$$

$$P_{ICB} = \int_{-\infty}^d p_2(z) dz$$

$$= \frac{1}{2} \operatorname{erfc} \left[\sqrt{\frac{1}{\frac{5}{4\gamma} + \frac{9}{4(K+1)}}}} \right]$$

$$\cdot \left(\frac{3}{2} \sqrt{\frac{K}{K+1}} - 1 \right) \quad (7b)$$

$$P_{ICC} = \int_d^{\infty} p_1(z) dz$$

$$= \frac{1}{2} \operatorname{erfc} \left[\sqrt{\frac{1}{\frac{5}{4\gamma} + \frac{9}{4(K+1)}}}} \right]$$

$$\cdot \left(1 - \frac{1}{2} \sqrt{\frac{K}{K+1}} \right) \quad (7c)$$

where γ is the ratio of the average signal power received to the noise power.

Letting P_{QCA} , P_{QCB} , and P_{QCC} be the error probabilities of the Q components for the 16 QAM signal for the first quadrant in Fig. 2, their error probabilities are equal to P_{ICA} , P_{ICB} , and P_{ICC} , respectively. Note that the I and Q components are statistically independent each other.

Thus, the total error performance of the 16 QAM signal points labelled S_1 , S_2 , S_3 and S_4 in Fig. 2 is given below;

$$P_I = P_{S1} + P_{S2} + P_{S3} + P_{S4}$$

$$= 4(P_{ICA} + P_{ICB} + P_{ICC}) \quad (8)$$

where P_{S1} , P_{S2} , P_{S3} and P_{S4} , are the error probabilities of 16 QAM signal points of S_1 , S_2 , S_3 and S_4 , respectively.

The average error performance with CTD in Rician fading environment is given below;

$$P_{EC} = \frac{4P_I}{16} = P_{ICA} + P_{ICB} + P_{ICC} \quad (9)$$

2. Optimum Threshold Detection(OTD)

We suggest that optimum threshold level(OTL) for the Rician fading channel is determined to be the point where $p_1(z) = p_2(z)$ on the I axis as

$$z_{opt} = \frac{3}{8} d \left[\frac{\sqrt{K} + \sqrt{K + \ln 3}}{\sqrt{1 + K}} \right] \quad (10)$$

Therefore, OTL are 0 and z_{opt} on the I axis. As mentioned previously, there are three cases when false detection of the 16 QAM signal is made if the I component of the transmitted 16 QAM signal is $d/2$ (2 cases) and $3d/2$ (1 case).

The error probabilities for the three cases are termed P_{IOA} , P_{IOB} , and P_{IOC} , respectively and they are specified in the following equations.

$$P_{IOA} = \int_{-\infty}^0 p_1(z) dz$$

$$= \frac{1}{2} \operatorname{erfc} \left[\sqrt{\frac{\gamma K}{5(1+K) + \gamma}} \right] \quad (11a)$$

$$P_{IOB} = \int_{-\infty}^{z_{opt}} p_2(z) dz$$

$$= \frac{1}{2} \operatorname{erfc} \left[\sqrt{\frac{1}{\frac{5}{4\gamma} + \frac{9}{4(K+1)}}}} \right] \cdot \left(\frac{3}{2} \sqrt{\frac{K}{K+1}} - B \right) \quad (11b)$$

$$P_{loc} = \int_{x_{0K}}^{\infty} p_1(z) dz$$

$$= \frac{1}{2} \operatorname{erfc} \left[\sqrt{\frac{1}{\frac{5}{4\gamma} + \frac{9}{4(K+1)}}}} \right] \cdot \left(B - \frac{1}{2} \sqrt{\frac{K}{K+1}} \right) \quad (11c)$$

where $B = \frac{3}{8} \left[\frac{\sqrt{K} + \sqrt{K + \ln 3}}{\sqrt{1 + K}} \right]$

Approaching similarly for the case of CTD, it is fairly easy to show that the average error performance of

16 QAM signal with OTD in the Rician fading environment becomes

$$P_{E0} = P_{IOA} + P_{IOB} + P_{IOC} \quad (12)$$

Figs. 4 and 5 illustrate the error performance of the 16 QAM signal in the Rician fading channel when CTD and OTD are selectively used in the demodulator. As shown in the figures when CNR = 30[dB] the error rate with CTD is 2×10^{-1} for $K = 5$ and 6.5×10^{-3} for $K = 30$. The error performance with OTD is 10^{-1} for $K = 5$ and 1×10^{-4} for $K = 30$. Thus, the performance with OTD is relatively better than that of CTD. However, to visualize the 16 QAM in a commercial system, a further improvement in its performance is necessary due to its inherently large error rate.

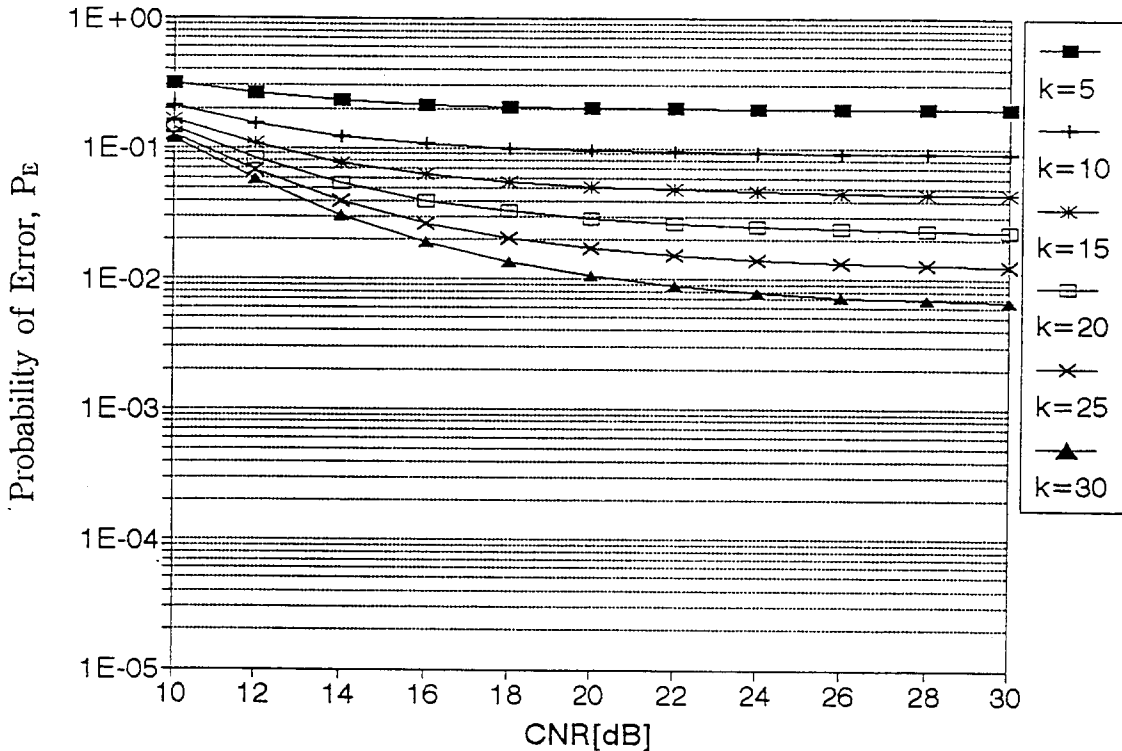


[Fig. 4] The error performance of 16 QAM signal with CTD in the Rician fading channel.

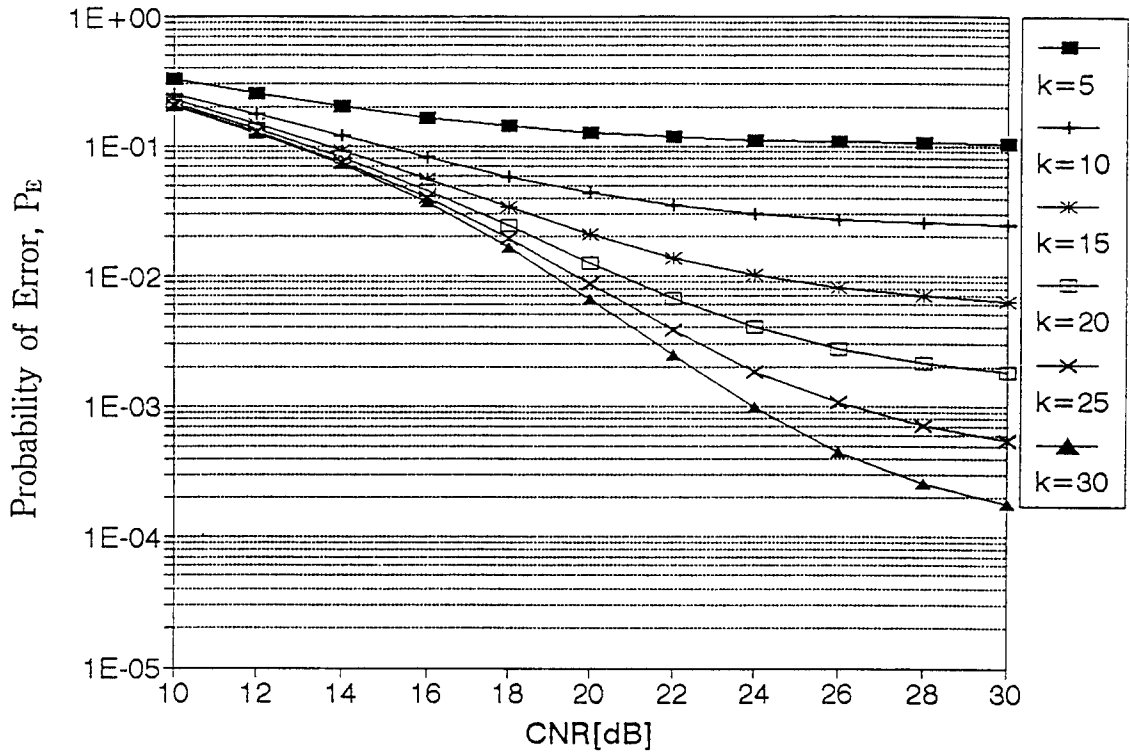


[Fig. 5] The error performance of 16 QAM signal with OTD in the Rician fading channel

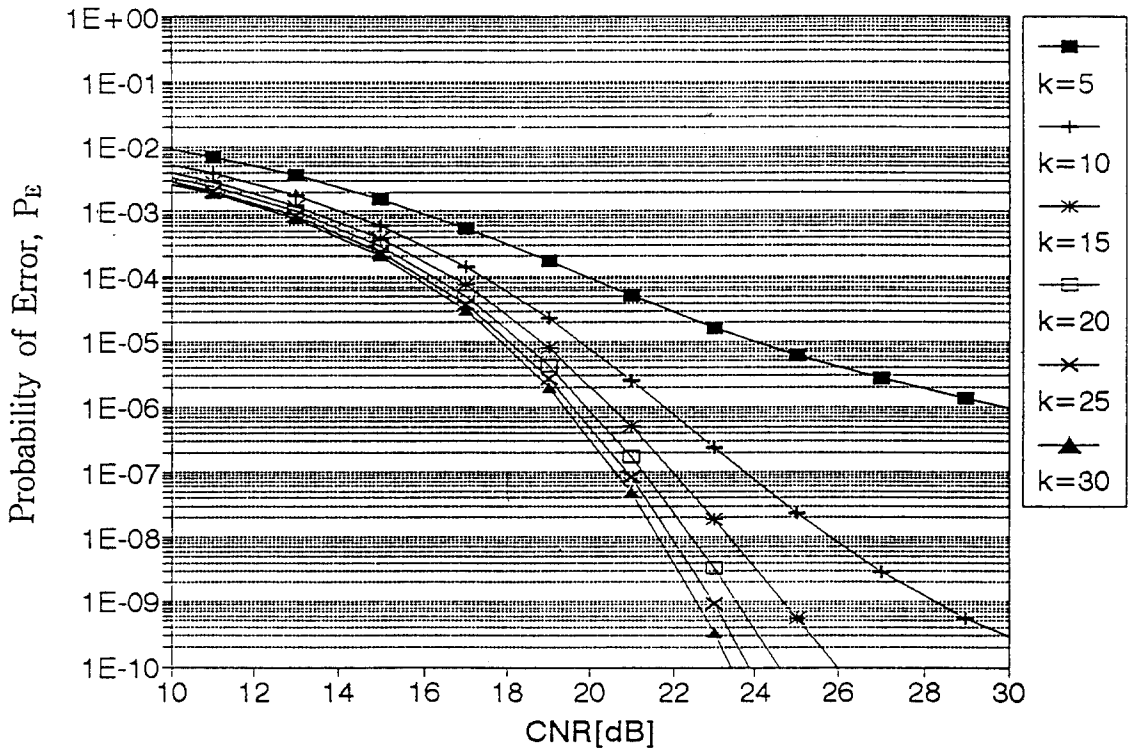


[Fig. 6] The error performance of 16 QAM signal with CTD in the Rician fading channel when SC diversity is adopted

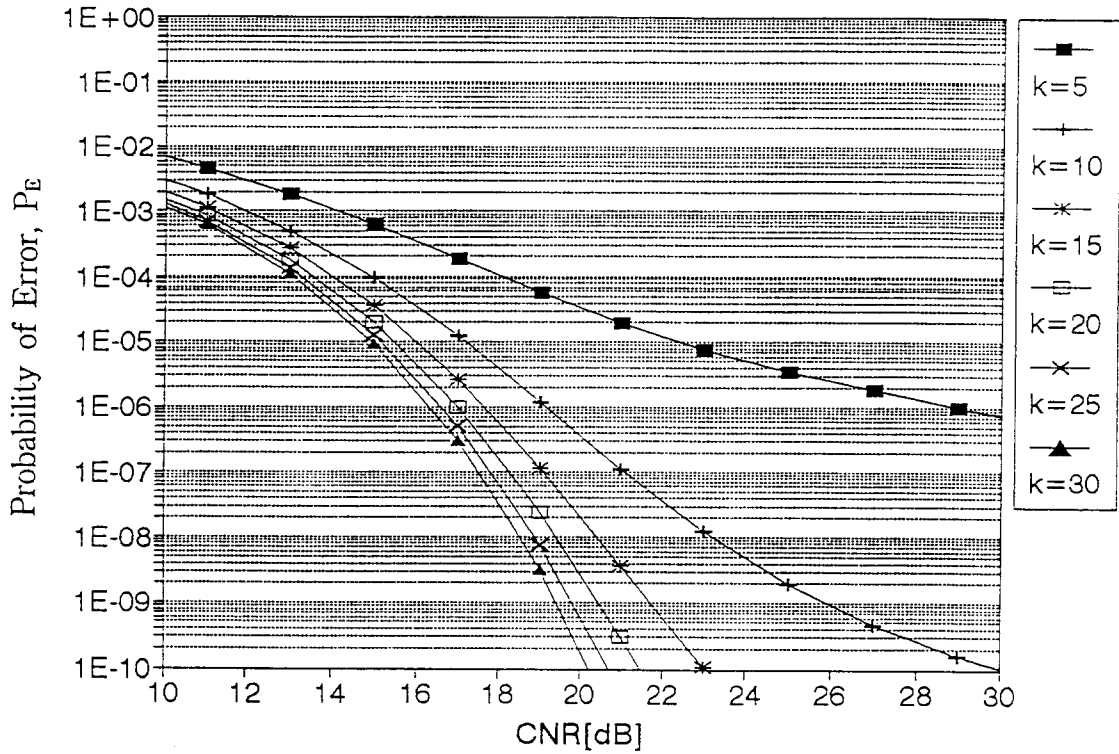


[Fig. 7] The error performance of 16 QAM signal with OTD in the Rician fading channel when SC diversity is adopted

IV. IMPROVEMENT OF ERROR PERFORMANCE BY DIVERSITY

The envelope of the received signal, r_i , corrupted by the Rician fading is Rician distributed as follows:

$$p(r_i) = \frac{r_i}{\Psi_0} \exp \left\{ -\frac{r_i^2 + A^2 R_0^2}{2\Psi_0} \right\} I_0 \left(\frac{r_i A R_0}{\Psi_0} \right) \quad (13)$$

where $I_0(\cdot)$ is the modified Bessel function of the first kind of order zero, $(AR_0)^2/2$ is the power of the direct component, and Ψ_0 is the power of the diffuse component.

By a simple change of variables in the pdf in the Eq. (13), we obtain the pdf of the instantaneous signal to noise ratio, $\gamma_i (= \frac{r_i^2}{2N})$, in the form

$$p(r_i) = \frac{K}{A^2 \Gamma} \exp \left\{ -\frac{K}{A^2 \Gamma} r_i - K \right\} \cdot I_0 \left(2\sqrt{\frac{K^2}{A^2 \Gamma}} r_i \right) \quad (14)$$

where $K = \frac{A^2 R_0^2}{2\Psi_0}$ and Γ is the average signal received to noise ratio ($= \frac{R_0^2}{2N}$).

Assuming that the received 16 QAM signal corrupted by the Rician fading in each diversity branch are uncorrelated, we derived the pdf of the instantaneous output signal to noise ratio, $p_M(\gamma_s)$, at the M-branch SC diversity reception circuit based on the procedure given in the reference[12]

$$p_M(\gamma_s) = M [1 - Q(\sqrt{2K}, \sqrt{\frac{2K}{\Gamma} \gamma_s})]^{M-1}$$

$$\begin{aligned} & \cdot \frac{K}{A^2\Gamma} \exp \left\{ -\frac{K}{A^2\Gamma} \gamma_s - K \right\} \\ & \cdot I_0 \left(2\sqrt{\frac{K^2}{A^2\Gamma} \gamma_s} \right) \end{aligned} \quad (15)$$

where $Q(a, b) = \int_b^{\infty} \exp \left\{ -\frac{(a^2 + x^2)}{2} \right\} I_0(ax) dx$.

The symbol error performance of 16 QAM signal with CTD and OTD is given in the Eqs. (16a) and (16b) respectively. They are obtained by integrating $P_c(\gamma_s)$, the error rate of CTD in AWGN and $P_o(\gamma_s)$, the error rate of OTD in AWGN over the density function of γ_s given in Eq. (15):

$$P_{E-SC} = \int_0^{\infty} P_c(\gamma_s) p_M(\gamma_s) d\gamma_s, \quad (16a)$$

$$\text{where } P_c(\gamma_s) = \frac{1}{2} \operatorname{erfc} \left[\sqrt{\frac{\gamma_s}{5}} \right]$$

$$P_{E-SC} = \int_0^{\infty} P_o(\gamma_s) p_M(\gamma_s) d\gamma_s, \quad (16b)$$

$$\begin{aligned} \text{where } P_o(\gamma_s) = & \frac{1}{2} \left\{ \operatorname{erfc} \left[\sqrt{\frac{\gamma_s}{5}} \right] \right. \\ & + \operatorname{erfc} \left[\frac{3}{4} \left(4 - \frac{\sqrt{K} + \sqrt{K + \ln 3}}{\sqrt{1 + K}} \right) \sqrt{\frac{\gamma_s}{5}} \right] \\ & \left. + \operatorname{erfc} \left[\frac{1}{4} \left(\frac{3\sqrt{K} + \sqrt{K + \ln 3}}{\sqrt{1 + K}} - 4 \right) \sqrt{\frac{\gamma_s}{5}} \right] \right\} \end{aligned}$$

The numerical evaluation of the Eqs. (16a) and (16b) is plotted in Figs. 6 and 7, respectively. The figures show that the error rate performance of the 16 QAM signal is well improved when the SC diversity is adopted. In fig. 6, when the error rate is 10^{-5} and $K = 5$, CNR is about 24.6[dB]. When $K = 30$, CNR is about 18.0[dB]. In fig. 7, when error rate is 10^{-5} and $K = 5$, CNR is about 22.8[dB]. When $K = 30$, CNR is about 15.2[dB]. Therefore,

when the SC diversity is adopted, we observed that OTD outperforms CTD by about 1.8~3.2[dB] when the error rate is 10^{-5} with $K = 5 \sim 30$.

V. CONCLUSIONS

We derived the optimum threshold level(OTL) for detecting 16 QAM signal, obtaining a better performance in the Rician fading channel than the conventional threshold detection(CTD). We derived the pdf of the instantaneous signal to noise ratio when the SC diversity is adopted. Observing the pdf's mentioned, we stated that adoption of the SC diversity brings a dramatic improvement of the error performance. Having the SC diversity reception, optimum threshold detection(OTD) technique proposed in this paper provides the performance improvement of 1.8~3.2[dB] in CNR for K values ranging from 5 to 30 over CTD when the error rate is 10^{-5} .

REFERENCES

1. D. J. Goodman, "Trends in cellular and cordless communications," IEEE Commun., Mag., pp.31-40, June 1991.
2. I. M. Ross and AT&T Bell Lab., "Wireless network directions," IEEE Commun., Mag., vol. 29, no.2, pp.40-42, Feb. 1991.
3. D. C. Cox, "Portable digital radio communications-An approach to tetherless access," IEEE Commun., Mag., vol.27, no.7, pp.30-40, July 1989.
4. N. Morinaga, S. Komaki and S. Hara, "Trends in modulation/demodulation and coding techniques for mobile satellite communications systems," IEICE(Japan) Trans. Commun., vol.E

- 74, no.8, pp.2211–2219, Aug. 1991.
5. S. Sampei, “Performance of trellis coded 16Q-AM/TDMA system for land mobile communications,” Proc. IEEE Globecom '90, pp.1953–1957, Dec. 1990.
 6. D. G. Brennan, “Linear diversity combining technique,” Proc. IRE, vol.47, pp.1075–1102, June 1959.
 7. J. G. Proakis, *Digital Communications*. 2nd ed., New York: McGraw-Hill, 1989.
 8. R. J. C. Bultitude, and G. K. Bedal, “Propagation characteristics on microcellular urban mobile radio channel at 910MHz,” IEEE J. on Selected Areas in Communication, vol.SAC-7, no.1, pp.31–39, Jan. 1989.
 9. A. M. D. Turkmani, J. D. Parsons, F. Ju, and G. Lewis, “Microcellular radio measurements at 900, 1500, and 1800MHz,” Proceedings of Fifth International Conference on Mobile Radio and Personal Commun., Coventry, UK, pp.65–68, Dec. 1989.
 10. A. B. Carlson, *Communication Systems*. 3rd ed., New York: McGraw-Hill, 1986.
 11. R. D. Gitlin, J. F. Hayes, and S. B. Weinstein, *Data Communications Principles*. New York: Plenum Press, 1992.
 12. M. Schwartz, *Communication Systems and Techniques*. New York: McGraw-Hill, 1966.